Physical Science International Journal

24(3): 9-19, 2020; Article no.PSIJ.55253
ISSN: 2348-0130

Characterization of Ka-band Radar Observations for Different Rain Types over Akure, Nigeria

Joseph S. Ojo[1], Babatunde A. Alabi[1*] and Moses O. Ajewole[1]

[1]Department of Physics, Federal University of Technology, Akure, Nigeria.

Authors' contributions

This work was carried out in collaboration among all authors. Author JSO designed the work, performed the statistical analysis, wrote the code and read the first draft of the manuscript. Author BAA wrote the first draft and managed the literature searches. Author MOA read the second draft and the analyses of the study. All authors read and approved the final manuscript.

Article Information

DOI: 10.9734/PSIJ/2020/v24i330180
Editor(s):
(1) Dr. Olalekan David Adeniyi, Federal University of Technology, Nigeria.
(2) Dr. Roberto Oscar Aquilano, National University of Rosario (UNR), Rosario Physics Institute (IFIR) (CONICET-UNR), Argentina.
Reviewers:
(1) Sara Pensieri, National Research Council of Italy, Italy.
(2) Ionac Nicoleta, University of Bucharest, Romania.
Complete Peer review History: http://www.sdiarticle4.com/review-history/55253

Review Article

Received 02 January 2020
Accepted 13 March 2020
Published 16 May 2020

ABSTRACT

Radar is a unique tool that can measure precipitation parameters over a large aerial coverage. Its application spans over study of climate change and radiowave propagation. Inter-relation between the rain parameters can also be derived with the height of radar especially on vertical profiling or aloft ground level. Hence effect of precipitation parameters can be assessed along the satellite propagation path with the help of space-borne radar. Satellite communication links operating at frequencies above 10 GHz are usually affected by hydrometeors especially rainfall. These effects are expected to be quite severe in the tropical region like Akure due to the nature of precipitation which is mainly convective and stratiform rain type. Therefore, information on vertical rain structure is important for precise quantitative estimation of precipitation. Thus, the focus of this work is to characterize the vertical profile of rain structures using vertically-pointing Ka-band Micro Rain Radar (MRR) at Akure, Nigeria. This has been achieved by using 2-year (2013 and 2014) data of rain parameters namely: rain rate, reflectivity, liquid water content and fall velocity obtained from MRR to determine the bright band heights under different rain types and its implications on satellite and radio waves propagation in this region. Rain rate in this region has been categorized into four groups namely: 0.02- 0.2 mm/h, 0.2- 2 mm/h, 2-40 mm/h, and 40 - 200 mm/h. The very low rain

**Corresponding author: E-mail: alabibabatunde4@gmail.com;*

rate group is related to the stratiform rain types whereas highest rain rate groups are for the convective rain type. Study shows that parameters that are much associated with rain attained peak value at different height depending on the period of the year. The vertical profile of Z shows peak around 3 to 4.2 km height. The peak region is associated with the bright band height and contribution to the melting layer. This study revealed that the occurrence of bright band heights varies with rain types. The overall results will be useful for determining rain height needed for the prediction of rain attenuation in this region.

Keywords: Ka-band; radar; micro rain radar; precipitation; bright band height; stratiform; convective.

1. INTRODUCTION

Rain has been identified as the most dominant factor that can cause degradations of millimeter wave signal. It plays a major role in the dreadful conditions of the communication links and if adequate measure is not taken it can lead to total signal loss. Other atmospheric effects also play their role in the design of satellite-to-earth, earth-to-satellite and terrestrial links operating at frequencies above 10 GHz [1]. Raindrops of different sizes for different rain types either absorb or scatter radio waves, leading to signal attenuation and reduction of the system availability and reliability. The severity of rain impairment increases with frequency and varies with regional locations [2]. Rain attenuation models are based on the properties of rain drops and interaction between rain drops and electromagnetic waves [3].

Recent studies revealed that incidence of rainfall on radio links become even more important for frequencies as low as about 7 GHz particularly in the tropical and equatorial climates, where intense rainfall events are common [4,5]. It is therefore very important when planning both microwave and terrestrial line-of-sight system links; to make an accurate prediction of rain induced attenuation on propagation paths. The uniqueness of vertically-pointing Radar is essential in this case especially the homogeneity in the stratiform rain type which is dominant in the region. Although convective rain occurs frequently as regard the tropical nature of the region, however stratiform rain is prevalent in the region with occurrence of about 56% per year [6,7].

Thus, the focus of this work is to characterize the vertical rain structure using a vertically-pointing Ka-band Micro Rain Radar (MRR) at Akure *(Lat 5°15'E, long 7°15'N)*, Nigeria. These characteristics are based on rain parameters such as rain rate, reflectivity, liquid water content and fall speed or velocity from Micro Rain Radar (MRR) to determine the melting layer and presence of bright band height (BBH) under different rain types.

2. EXPERIMENTAL SETUP

This research utilizes 2-year (2013 and 2014) rainfall parameters data obtained from a vertically-pointing Ka-band radar (MRR) located at the Department of Physics, Federal University of Technology Akure (FUTA) *(Lat 5°15'E, long 7°15'N)*. The climatic condition of Akure is influenced by the rain-bearing southwest monsoon winds which emanated from the Ocean and the dry northwest winds from the Sahara Desert. Akure experiences a warm humid tropical climate, with two distinct seasons namely: the rainy and dry seasons. The rainy season lasts for about seven months, April to October while the dry season months span from November to March of the succeeding year. The city has an average annual rainfall of about 1485.57 mm with a short August break The average temperature is about 22°C during Harmattan (December to February) and 32°C in March [1]. Fig. 1 presents the map of FUTA showing where the data was collected. The evidence of strong rain attenuation at MRR frequency (26.1 GHz) cannot be underrated, so also the vertical wind that affect the fall speed of the drop [8] most especially during heavy rainfall. However, adequate correction has been adopted by meteorological mess technique GmbH (METEK) with provision of software which has been applied to our instrument [9]. A brief description of the instrument and mode of data processing is presented in the sub-section below.

2.1 Instrumentation

The basic equipment used for the study is the vertically-pointing MRR with an operating frequency of 24.1 GHz. The outdoor and indoor unit of the MRR is presented in Fig. 1 respectively. The MRR antenna is

simultaneously used for the transmission of the RADAR signals and receiving of backscattered signals from the raindrops. It is designed as an offset parabolic dish. The angular aperture is approximately 2°. The parabolic dish is fastened together with the electronics unit and the RADAR module through the antenna mounting. The use of a parabolic dish allows a vertical alignment of the antenna beam without the need of a horizontal alignment.

The antenna is positioned so as to allow rainwater drain off without retaining it. The electronics unit shown in Fig. 2(a) generates the RADAR transmitting signal and passes it to the RADAR module. It analyses the backscattered received signal and transfers the data to the connected control and evaluation computer, where the Doppler spectra are computed. The electronics unit is located in a water protected IP65 housing, which is fixed to the antenna mounting. At the bottom side of the electronics unit there is a socket for the cable leading to the connection box/power supply. The connection box with the aid of a 25-pin D-sub-miniature socket female type is used to pass the data through to the controlling computer as shown in Fig. 2(b). A flanged socket is used for connecting RADAR electronics unit box to the connection box, the power supply is also integrated in the connection box. The vertical profile of the rain rate, liquid water content, fall velocity and radar reflectivity factor are based on time resolution of 10 seconds and the rain height resolution fixed at 160 m stepwise up to 4.8 km in 30 steps. The rain event of the 10 seconds is integrated over one minute. The MRR samples the fall velocities of the precipitation particles to deduce the drops size distributions (DSD), rain rate, liquid water content and radar reflectivity from the fall velocity spectrum [10,9,6]. The following expression relates the rain parameters [10,11].

2.1.1 Equivalent radar reflectivity factor

The equivalent radar reflectivity factor *Z* is defined as:

$$Z = \int_0^\infty N_v(D)D^6 \mathrm{dD} \quad (1)$$

where $N_v(D)D^6$ (the subscript *v* standing for volume) represents the mean number of raindrops with equivalent spherical diameters between D and D+dD (mm) present per unit volume of air. The corresponding units of $N_v(D)D^6$ is $mm^{-1}m^{-3}$.

2.1.2 Rain drop size distribution model

This is derived by MRR algorithm using lognormal distribution model.

A general form of the three parameter distribution is given by Ajayi and Barbaliscia [12]:

$$N(D)=\frac{N_T}{\sigma D\sqrt{2\pi}} exp[-\frac{1}{2}\{\frac{In(D)-\mu}{\sigma}\}^2]\ mm^{-1}m^{-3} \quad (2)$$

where N (D) is the number of drops per unit volume per diameter interval, μ is the mean *In (D)*, σ is the standard deviation, D as drop diameter and N_T is the total number of drops of all sizes.

2.1.3 Liquid water content based on DSD

The liquid water content is the product of the total volume of all droplets with the density of water ρ_w, divided by the scattering volume. It is therefore proportional to the third moment of the drop size distribution. This is calculated by using:

$$Lwc = \rho_w, \frac{\pi}{6}\int_0^\infty N\ (D)\ D^3 dD \quad (3)$$

2.1.4 Rain Rate based on DSD

This is the rate at which water reaches the ground or the rate of accumulation of water per unit time (mm/h). The differential rain rate is equal to the volume of the differential droplet number density multiplied with the terminal falling velocity *v(D)* [13]:

$$v(D)\ = \left(\frac{\pi}{6}N(D)D^3\right) \quad (4)$$

where N (D) is the number of drops per unit volume per diameter interval and D is the drop diameter. From equation (4) the rain rate was obtained by integrating over the drop size as:

$$RR=\frac{\pi}{6}\int_0^\infty N\ (D)\ D^3 v(D) dD \quad (5)$$

2.2 Data Pre-processing

The data comprises of rainfall parameters, namely: rain rates, radar reflectivity, liquid water content and fall velocity; based on vertical profiles. Basically rain rate in this region is categorized into convective and stratiform using the following single criterion. The mean vertical profiling of rain are grouped into four rain rate groups namely; 0.02-0.2 mm/h (drizzle),

0.2-2 mm/h (widespread), 2.0-40 mm/h (shower), 40-200 mm/h (thunderstorm). After processing, the number of profiles in the rain rate region of 0.02-0.2 mm/h is 32,432, in 0.2-2 mm/h are 37,252, in 2.0-40 mm/h are 18,242 and in 40-200 mm/h are 825.

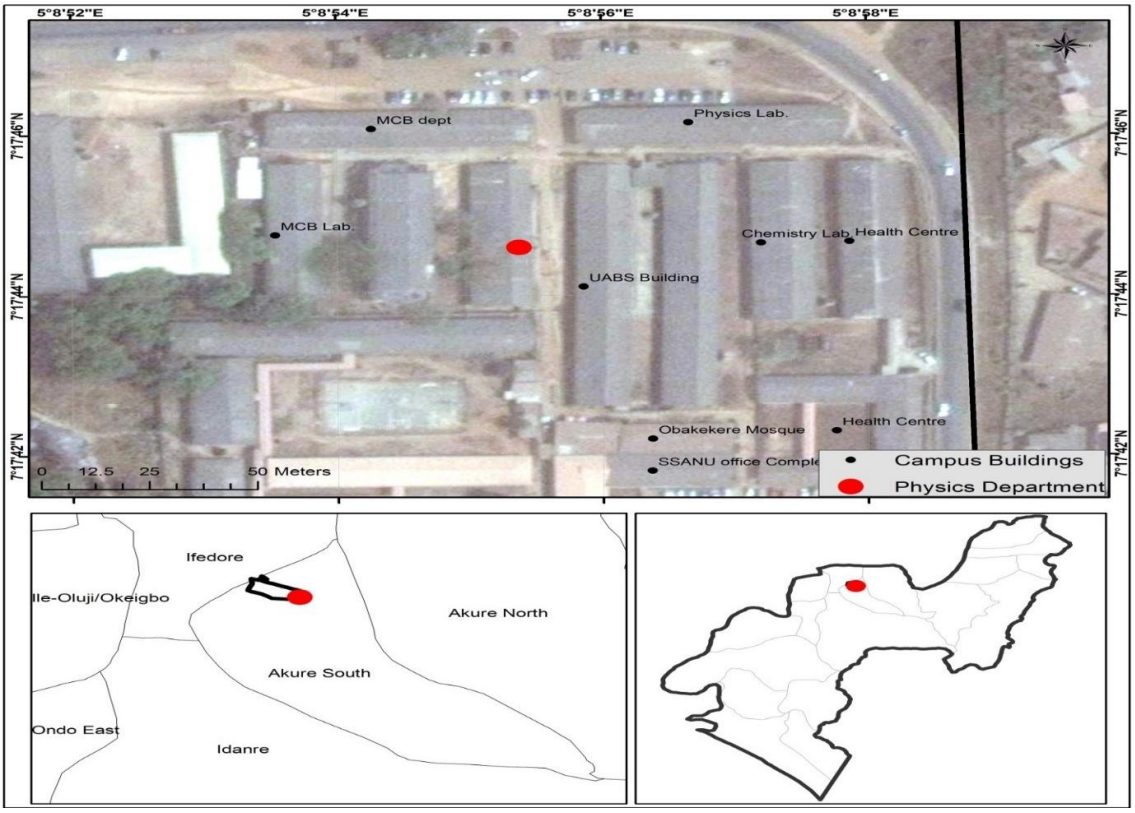

Fig. 1. Map of F.U.T.A., Akure Ondo State, Nigeria showing where data was collected

(a) (b)

Fig. 2. The MRR (a) outdoor and (b) indoor units

3. RESULTS AND DISCUSSION

3.1 Average Vertical Profile of Rainfall Parameters at Different Rain Types

In order to understand the variability of the rain structure under different rain types, the profiles of rain rate (RR), liquid water content (LWC), fall speed (W), and radar reflectivity (Z) for different rain classes as shown in Figs. 3 - 5 for the months of November 2013, April 2014, June 2014 and September 2014 respectively were studied. These months were chosen because they represents the beginning of dry season months, commencement of rainy season months, stratiform period and commencement of convective rainy period respectively. For example Fig. 3 (a-d) shows the average vertical profile of rainfall parameters under different rain types for Z, LWC, W, and RR respectively. The result is presented for the month of November 2013 representing the beginning of dry season months. A typical result of Z- profiling (Fig. 3a) shows that the peak was found around 4.2 km. Peak in this context relatively means the region with conspicuous protruding to the right. This region represents the bright band height (BBH) as reported in the work of Das et al. [14]. BBH usually occurs near the zero degree isotherms which in this case is around 4.2 km. The enhancement of reflectivity around 4.2 km is thus contributed to the presence of the melting layer, this indicates that the formation of bright band occurs around 4.2 km level with embedded small scale convective activity for the month under consideration. A smaller peak is also visible around 2.0 km which may be cause by liquid rain. The maximum intensity corresponding to

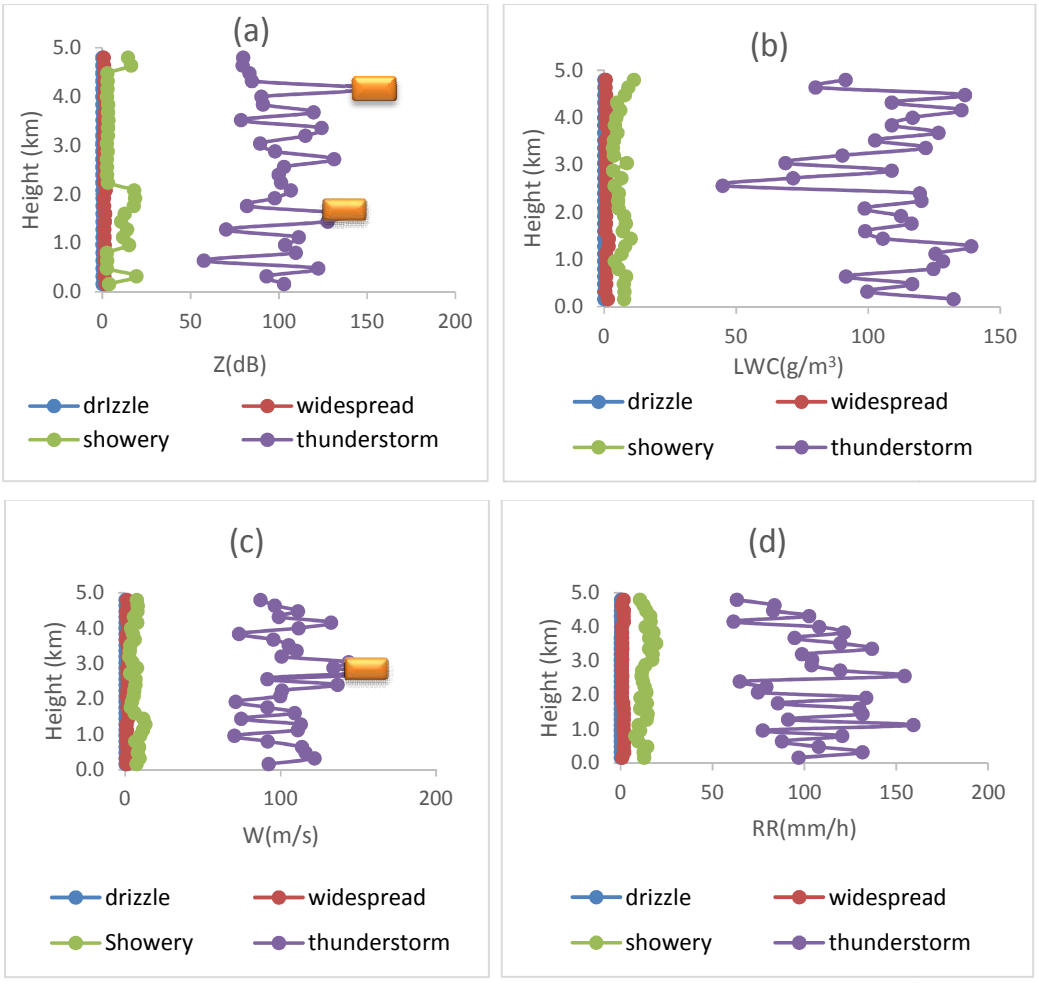

Fig. 3. Average vertical profile of rainfall parameters for the month of November 2013 under different rain types for (a) Z (b) LWC, (c) W and (d) RR respectively

the liquid rain occurs at lower height may also be due to convective process [11,15]. Similar trend could be observed for the vertical profile of LWC as indicated in Fig. 3(b). The average fall velocity also shows a broader peak at 3.0 km (Fig. 3c). This event correspond to a mixture of the convective type with stratiform type rain as pointed out by Steiner et al. [16] and Awaka et al. [17]. In Fig. 3 d for the rain rate events, clear bright band could not be seen since the indicated month represents the commencement of dry season months. The dry season month is associated with little or no rain.

Fig. 4 (a-d) also presents the average vertical profile of rainfall parameters under different rain types for Z, LWC, W, and RR respectively. The results are presented for the month of April 2014 representing the commencement of rainy season months.

The description of the event follows same trend as discussed for Fig. 3 (a-d), however with a little different in the position of bright band. For example, the reflectivity profile in Fig. 4(a) shows no clear evidence of melting layer due to the convective nature of the rain types. Earlier studies show that the commencement of rainy season in Nigeria is usually associated with convective rain types [1].

However, other rain parameters LWC, W and RR in Fig. 4(b-d) shows evidence of peaks around 4.5 km heights. These indicated the presence of bright band, although not so conspicuous except for the plot for the RR (Fig. 4d). This might be due to the presence of heavy rainfall at the commencement of rainy season. Similar trend could be observed in Fig. 5(a-d) for the month of June, representing the intense stratiform period, although, the evidence of the bright band is not as conspicuous as that of Fig. 3.

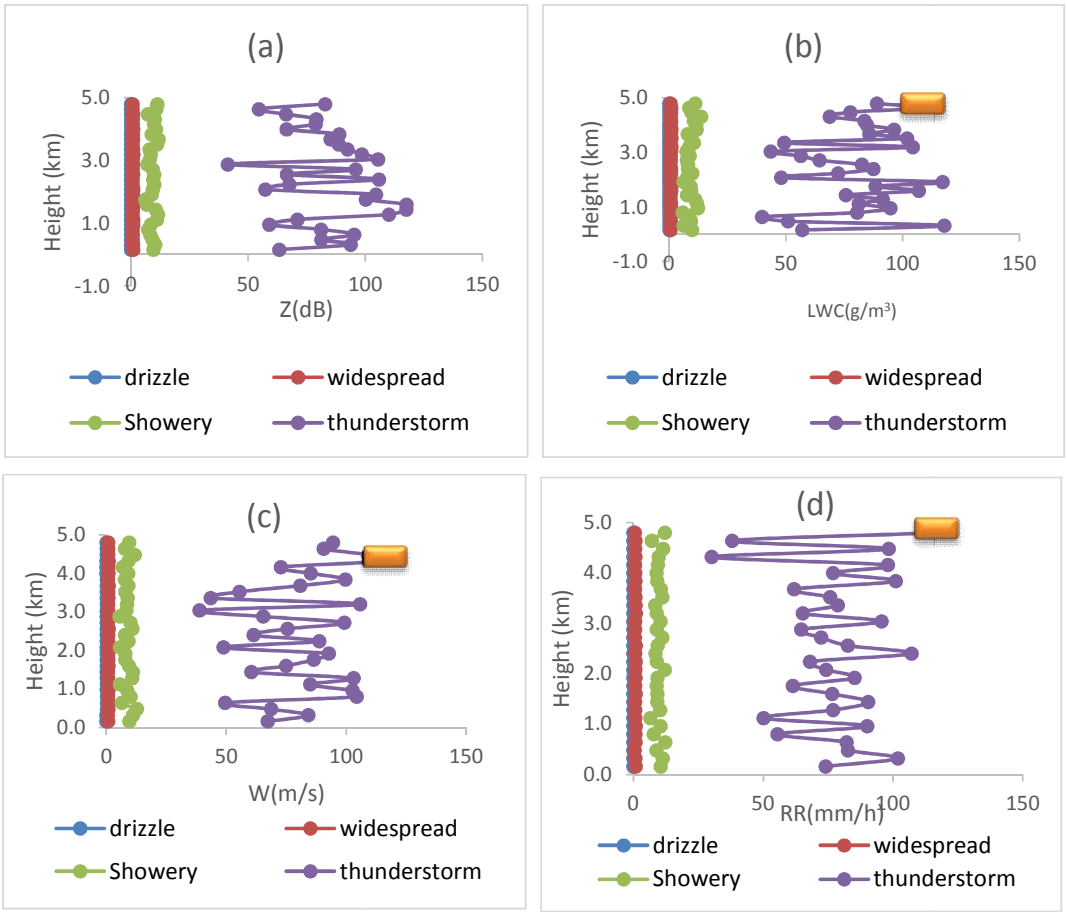

Fig. 4. Average vertical profile of rainfall parameters for the month of April 2014 representing the commencement of rainy seasons under different rain types for (a) Z, (b) LWC, (c) W, and (d) RR respectively

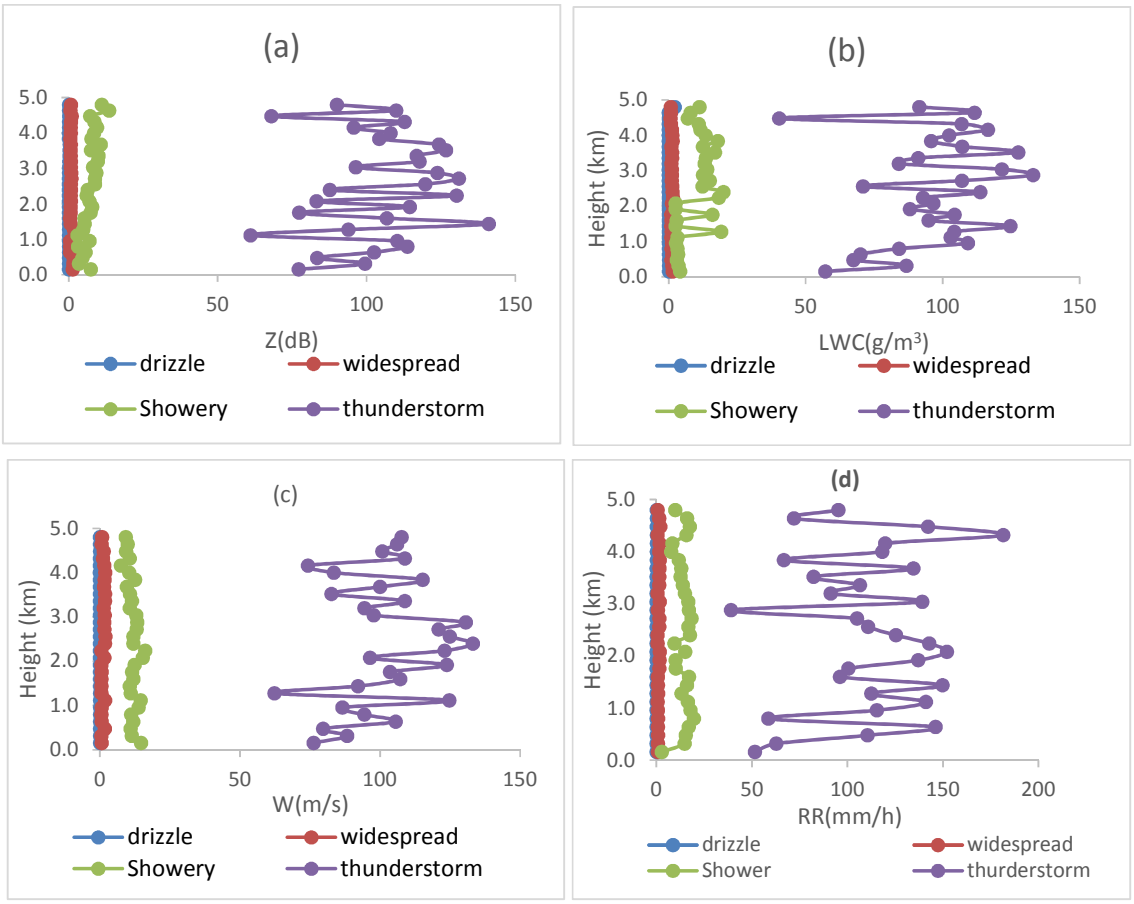

Fig. 5. Average vertical profile of rainfall parameters for the month of June 2013 representing the stratiform period under different rain types for (a) Z, (b) LWC, (c) W, and (d) RR respectively

Fig. 6 (a-d) also presents the average vertical profile of rainfall parameters under different rain types for Z, LWC, W, and RR respectively for the month of September 2014 which represents the commencement of the convective rainy period.

In Fig. 6 (a) for example, radar reflectivity profile Z shows a peak at around 3.0 km height which indicates that the rain type is stratiform [18], Reflectivity Z and LWC profiles as presented in Fig. 6 (a) and 6 (b) show almost uniform structure with heights. They both have corresponding melting layer around 3.0 km height which indicate the events as stratiform. A smaller but broader peak is also visible around 4.0 km in Fig. 6 (c) which may be caused by liquid rain. This indicates that the formation of bright band occur around 4.0 km with small scale convective activity however Fig. 6 (d) for rain rate profile shows that no bright band is present, indicating that the rain type is convective. These results indicated that BBH can occur at any heights above 3 km for these months.

3.2 Stratiform and Convective Events

Stratiform (0.02 - 0.2 mm/h, 0.2 - 2 mm/h) and convective (2-20 mm/h and 20-200 mm/h), events are presented in Figs. 7 (a-b) and 8(a-b) respectively. Here, some typical rain event observed on 26 June 2014 occurring from 16.41.27 LT to 23.59.28 LT and 06 September 2014 occurring from 01.22.34 LT to 23.59.00 LT are presented. The time series of vertical reflectivity of MRR is studied for different rain events (stratiform and convective) based on rain rate categorization. The very low rain rate group is related to the definite stratiform rain whereas the highest rain rate group designates the definite convective rain. Once the

bright band is observed in the profile, a more in depth study in terms of different parameters is performed. The stratiform rain is more uniform vertically than the convective rain up to the melting layer height. The band-like structure is clearly observed for the selected days at about 4.5 km for the radar reflectivity as presented in Fig. 7 (a and b).The band-like structure seen around 4.5 km as shown in Fig. 7 (a) in radar reflectivity is due to the presence of melting layer called radar bright band as discussed earlier. The same trend could be observed in Fig. 7(b) which shows rains under this class are of stratiform event (0.02 - 0.2 mm/h, 0.2 - 2 mm/h).

The vertical profiles for the convective rain types (2-20 mm/h and 20-200 mm/h), as observed by MRR is also shown in the Fig. 8 (a-b) for the rain event on 15 September 2014 and 19 September 2014 respectively. Radar reflectivity profile is presented for 00:03:13 to 22:34:30 LT which shows that no bright band is present and the rain type is convective [18]. The convective rain is associated with vertical wind motion prohibiting formation of melting layer.

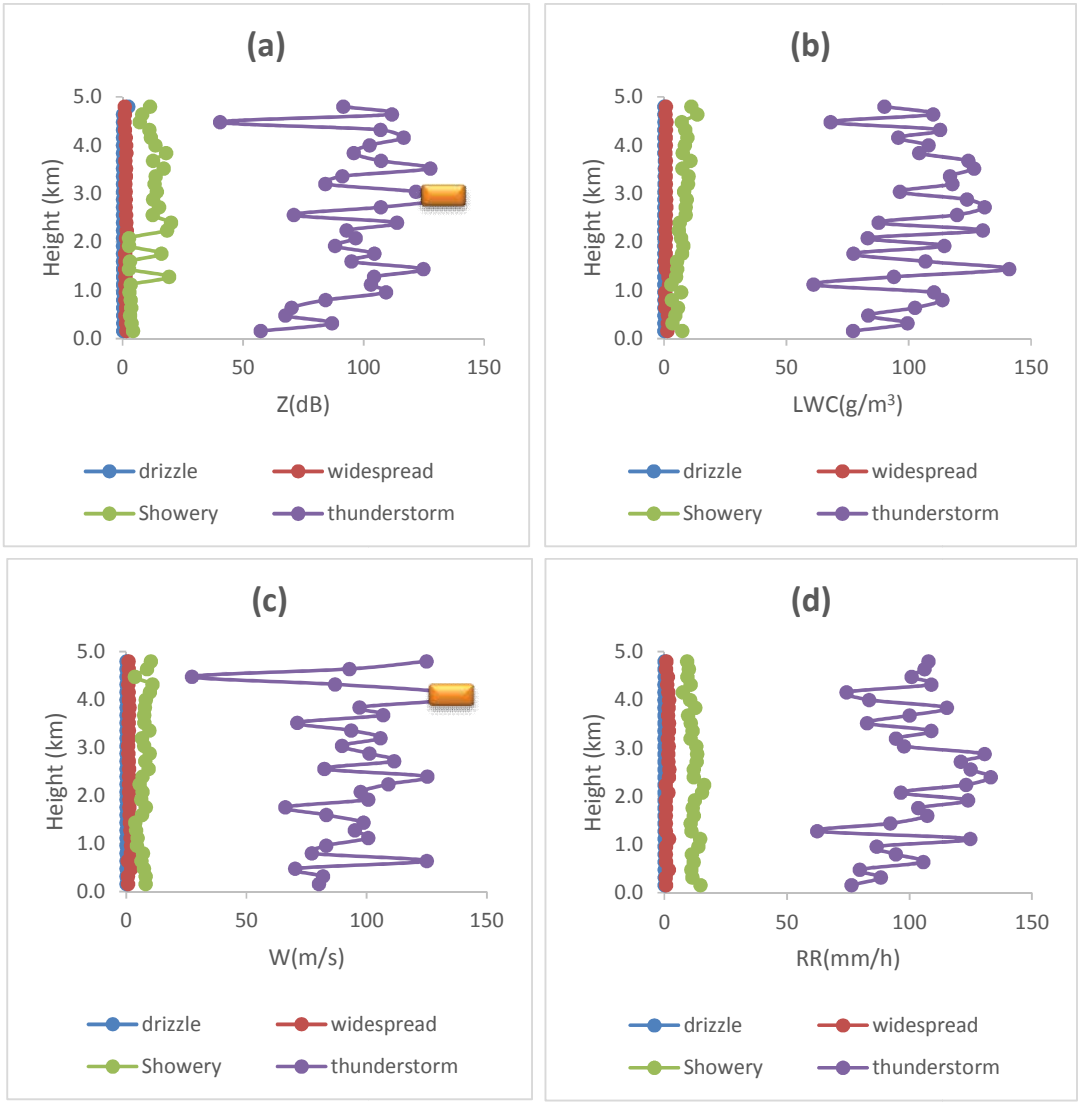

Fig. 6. Average vertical profile of rainfall parameter for the month of September 2014 representing commencement of convective rainy period under different rain types for (a) Z, (b) LWC, (c) W and (d) RR

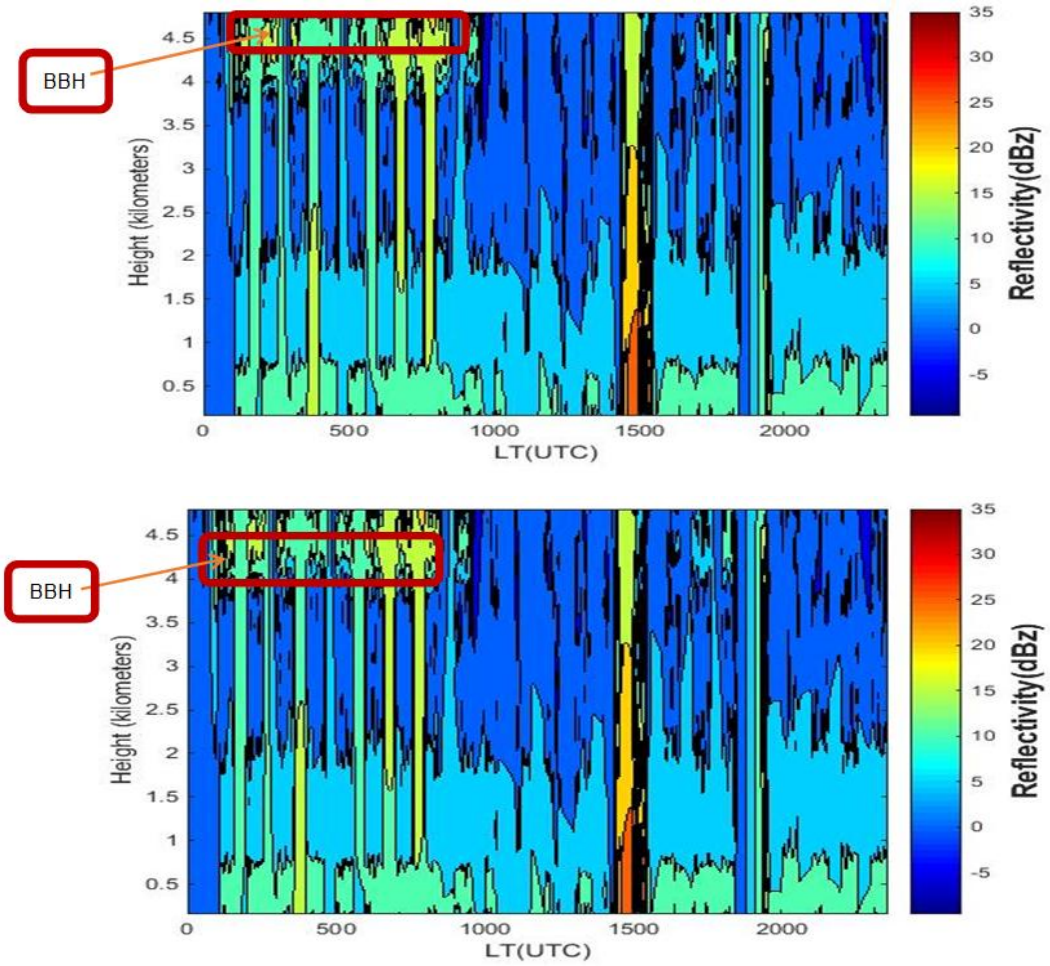

Fig. 7. Radar reflectivity profile for (a) 16.41.27 LT to 23.59.28 LT on the 26/06/2014; (b) 01.22.34 LT to 23.59.00 LT on the 06/09/2014

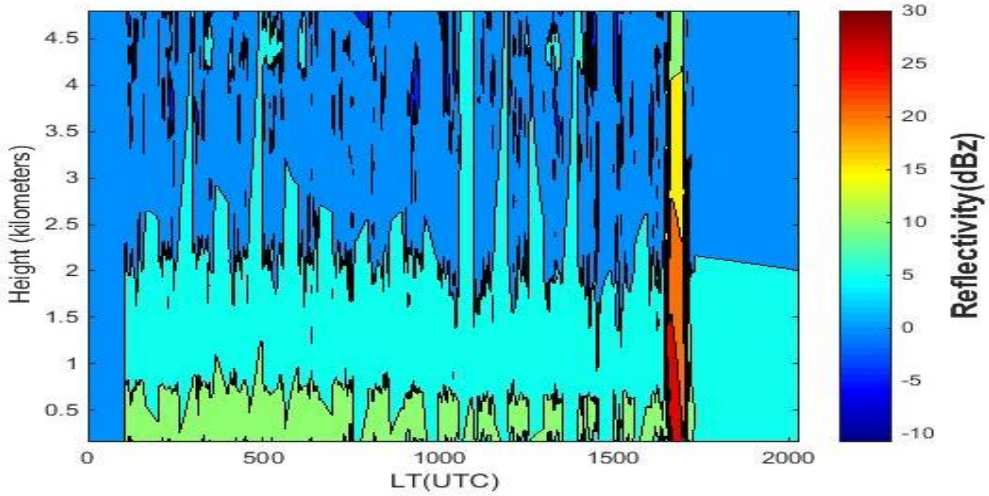

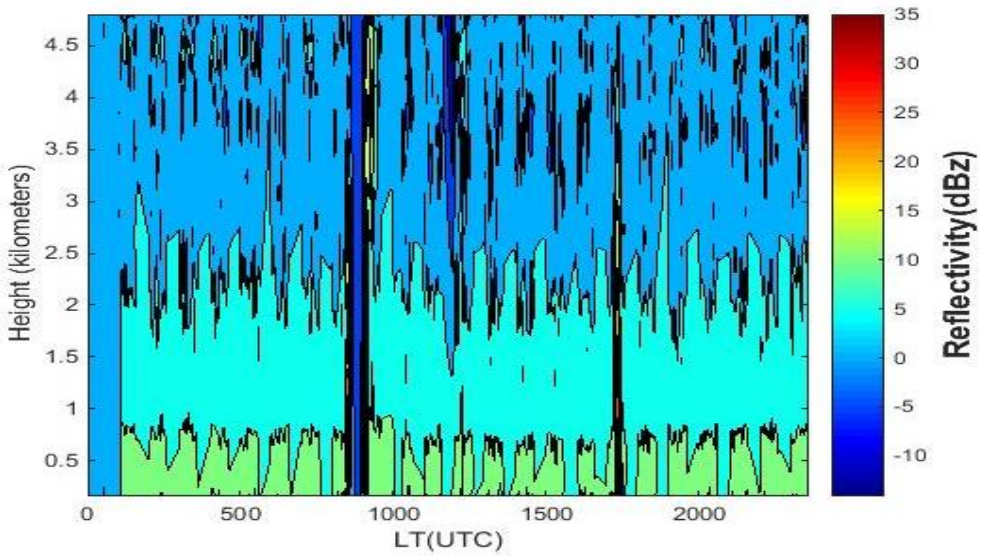

Fig. 8. Radar reflectivity profile of (a) 15/09/2014 for 00:03:13 to 22:34:30 LT (b) 19/09/2014 for 01:00:00 – 23:00:00 LT

4. CONCLUSION

This paper has presented recent study on the profile of Ka-band radar observations for different rain types in a tropical location. The study has been based on the characterization of rain parameters namely: radar reflectivity (z), liquid water content (LWC), fall velocity (w), and rain rate (RR) measured using vertically pointing micro rain radar in Akure, Nigeria. In each rain parameters, bright band height has been deduced based on melting layer. The measurements of the bright band allow us to derive the dependence of bright band characteristics on rain type and intensity which help to quantify the contribution of the various causes to the bright band signature. The stratiform rain event shows maximum value of a clear bright band around 4.5 km in reflectivity profile. In contrast, the convective rain has no bright band in such height due to the strong wind motion characterized by the convective activity. The fall velocity and radar reflectivity also show significantly varied vertical profile at different rain types. Melting layer signature in Z-profile is obtained around 4.5 km in rain rate ranges 0.2–2 mm/h and indicates that most of the rain in this region is of stratiform type. However, in the 20–200 mm/h rain class does not show such bright band and essentially represents the convective rain structure. Generally the study revealed that the occurrence of BBH varies with rain parameters and with rain types.

ACKNOWLEDGEMENTS

Authors wish to acknowledge the support of Communication Research group of Physics Department, FUTA, Nigeria for providing data used for this study.

COMPETING INTERESTS

Authors have declared that no competing interests exist.

REFERENCES

1. Ojo JS, Olurotimi EO. Tropical rainfall structure characterization over two stations in Southwestern Nigeria for radiowave propagation purposes. Journal of Emerging Trends in Engineering and Applied Sciences. 2014;5(2):116–122.
2. Chebil J, Rahman TA. Development of 1 min rain rate contour maps for microwave applications in Malaysia Peninsula. Electronics Letts. 1999;35:1712–1774.
3. Crane RK. Prediction of the effects of rain on satellite communication system. Proceedings of the IEEE. 1977;65:456–474.
4. Moupfounma F. Rainfall-rate distribution for radio system design. IEE Proceedings. 1997;134:527-537, Pt. H, No. 6.
5. Ojo JS, Ajewole MO, Sarkar SK. Rain rate and rain attenuation prediction for satellite

communication in Ku and Ka bands over Nigeria. Prog Electromagn Res B (Hong Kong). 2008;207-223.

6. Marzuki, Hashiguchi H, Kozu T, Shimomai T, Shibagaki Y, Takahashi Y. Precipitation microstructure in different Madden-Julian Oscillation phases over Sumatra. Atmos. Res. 2016;168:121–138.
7. Ojo JS, Tomiwa AC, Ajewole MO. Characterization of vertical profile of rain microstructure using micro rain radar in a tropical part of Nigeria. Physical Science International Journal. 2018;18(1):1-12. Article no.PSIJ.36981.
8. Tridon F, Baelen JV, Pointin Y. Aliasing in micro rain radar data due to strong vertical winds. Geophys. Res. Lett. 2011;38: L02804.
   DOI: 201110.1029/2010GL046018
9. Peters G, Fischer B, Clemens M. Rain attenuation of radar echoes considering finite-range resolution and using drop size distributions. J. Atmos. Ocean. Technol. 2010;27:829–842.
10. Peters G, Fischer B, Münster H, Clemens M, Wagner A. Profiles of raindrop size distributions as retrieved by micro rain radars. J. Appl. Meteorol. 2005;44:1930–1949.
11. Gerhard P, Fischer B, Münster H, Clemens M, Wagner A. Profiles of raindrop size distributions as retrieved by micro rain radars. Journal of Applied Meteorology. 2005;44:1930–1949.
12. Ajayi GO, Barbaliscia F. Prediction of attenuation due to rain: Characteristics of the 0°C isotherm in temperate and tropical climates. Int. J. of Sat. Comm. 1990;8:187-196.
13. Oluwadare EJ, Tomiwa AC, Ajewole MO. Investigation of Radiowave propagtion impairment at super high frequency due to Rain in Akure. American International Journal of Contemporary Research 2012;2(10):122. Rainfall estimates in stratiform rain. Weather Forecast. 23;1085–1101.
14. Das S, Shukla AK, Maitra A. Investigation of vertical profile of rain microstructure at Ahmedabad in Indian tropical region. Adv. Space Res. 2010;45(10):1235-1243.
    Available:http://dx.doi.org/10.1016/j.asr.2010.01.001
15. Thurai M, Deguchi E, Okamoto K, Salonen E. Rain height variability in the tropics. IEE Proc. Microw. Antennas Propag. 2012;152(1):17-23.
16. Steiner M, Houze Jr. RA, Yuter SE. Climatological characterization of three-dimensional storm structure from operational radar and rain gauge data. J. Appl. Meteor. 1995;34:1978–2007.
    DOI: 10.1175/1520-0450(1995)034,1978: CCOTDS.2.0.CO;2.
17. Awaka J, Iguchi T, Okamoto K. Early results on rain type classification by the tropical rainfall measuring mission (TRMM) precipitation radar. Proc. 8th URSI Commission F. Open Symp. Aveiro, Portugal. 1998;143-146.
18. Williams CR, Ecklund WL, Gage KS. Classification of precipitating clouds in the tropics using 915–MHz wind profilers. J. Atmos. Ocean. Tech. 1995;12:996–1012.

Peer-review history:
The peer review history for this paper can be accessed here:
http://www.sdiarticle4.com/review-history/55253